Volume 293, number 1,2, 53–58 FEBS 10381 November 1991

Photooxidation of high-potential (c_{559}, c_{556}) and low-potential (c_{552}) hemes in the cytochrome subunit of *Rhodopseudomonas viridis* reaction center

Characterization by FTIR spectroscopy

E. Nabedryk[1], C. Berthomieu[1], A. Verméglio[2] and J. Breton[1]

[1]*DBCM/SBE, CEN Saclay, 91191 Gif-sur-Yvette, France* and [2]*DPVE/SBC, CEN Cadarache, 13108 St Paul lez Durance, France*

Received 3 August 1991; revised version received 23 September 1991

The photooxidation of c_{559}, c_{556} and c_{552} hemes in *Rhodopseudomonas viridis* cytochrome has been characterized by light-induced FTIR difference spectroscopy. Apart from the common features at 1659 cm^{-1} and 1561/1551 cm^{-1} which could arise from one (or possibly two) peptide bond(s), no evidence for major structural rearrangement of the polypeptide backbone was observed. A significant difference with respect to redox-induced FTIR spectra of cytochrome *c* is the absence of the Tyr marker at 1514/1518 cm^{-1} in *Rps. viridis* cytochrome, indicating that the localized shift of a Tyr side chain observed between ferro- and ferri-cytochrome *c* does not occur in *Rps. viridis* cytochrome.

Fourier transform infrared spectroscopy; Bacterial reaction center; Photosynthesis; Cytochrome; *Rhodopseudomonas viridis*

1. INTRODUCTION

The reaction center (RC) from the purple bacteria *Rhodopseudomonas viridis* contains a tightly bound tetraheme cytochrome (cyt) which functions as an electron donor [1,2] to the photooxidized primary electron donor (P). Two of the hemes are high-potential and two are low-potential. The spatial alignment of the 4 hemes has been revealed by X-ray analysis of the RC crystal [3,4]while their respective assignment, in terms of redox potentials, has been inferred from spectroscopic and fast kinetic studies [5–9]. In particular, it has been established that the c_{559} high-potential heme is the closest one to P. The sequence of the 4 hemes as well as their respective mid-point potentials are the following [5–10]: c_{559} (heme 3), 360 mV; c_{552} (heme 4), 20 mV; c_{556} (heme 2), 310 mV; c_{554} (heme 1), −60 mV. At room temperature, at a redox potential at which all 4 hemes are oxidized in the dark, and in the absence of electron transfer from the primary quinone acceptor Q_A to the secondary quinone Q_B, the $P^+ Q_A^-$ state generated under illumination recombines in about 1 ms [11]. When the two high-potential hemes are reduced in the dark, a flash induces the rapid oxidation of c_{559} by the photogenerated P^+ ($t_{1/2}\approx300$ ns) which is followed by a slower electron transfer from c_{556} to c_{559} ($t_{1/2}\approx3$ μs) [1,12]. When c_{552} is reduced, its oxidation by P^+ is also very rapid ($t_{1/2}<1$ μs) [2]. The back-reactions between Q_A^- and the oxidized c_{559} and c_{556} hemes have been measured to be of the order of 100 ms and 1 s, respectively [12]. In addition to this functional unequivalence of the hemes with respect to the kinetics of electron transfer, crystallographic data have shown that the 4 Fe-porphyrins are in different protein surroundings in the single cyt subunit [4]. Each heme is covalently linked to two Cys residues via thioether bonds with the typical sequence of the heme binding segment found in all *c*-type cyt, Cys-X-X-Cys-His, with the His residue as the fifth ligand to the heme iron. The sixth ligand for c_{552} is also His [4] while it is Met for all other hemes.

Light-induced FTIR difference spectroscopy is an attractive tool to follow the structural and functional changes accompanying charge separation and stabilization during primary reactions in photosynthetic bacteria [13 and references therein]. Specific IR changes occuring upon the $PQ_A \rightarrow P^+Q_A^-$, $PQ_B \rightarrow P^+Q_B^-$, $Q_A \rightarrow Q_A^-$ and $Q_B \rightarrow Q_B^-$ transitions have been recently characterized in *Rps. viridis* RC and chromatophores [14–19]. In addition, the combination of FTIR difference spectroscopy and electrochemistry has been successfully applied to monitor redox-linked conformational changes in cyt *c* from several species [20]. Here, we report on distinct light-induced FTIR difference spectra obtained with *Rps. viridis* RC upon photooxidation of either c_{559} or c_{556} or c_{552} heme. Molecular struc-

Abbreviations: FTIR, Fourier transform infrared spectroscopy; RR, resonance Raman; VIS, visible; cyt, cytochrome; P, primary electron donor; RC, reaction center; Q_A (Q_B), primary (secondary) quinone electron acceptor.

Correspondence address: E. Nabedryk, DBCM/SBE, Bât 532, CEN Saclay, 91191 Gif-sur-Yvette Cedex, France. Fax: (33) (1) 6908 8717.

tural changes accompanying cyt oxidation at the level of both heme and protein groups are compared between high- and low-potential cyt.

2. MATERIALS AND METHODS

Preparation of *Rps. viridis* RC samples for IR spectroscopy was carried out as in [18]. Before complete drying of the RC solution in cholate on a CaF_2 disc, it was covered with 7 μl of a 20 mM Tris buffer, pH 7, containing 5 mM *o*-phenanthroline and, if necessary, redox compounds (diaminodurene, sodium ascorbate). The sample was sealed with another CaF_2 window when the final aqueous volume was $\approx$3 μl, leading to an estimated RC concentration of 2–5 mM.

Light-induced IR, near-IR and visible (VIS) measurements at 10°C were performed alternately on the same sample under identical geometry, using a Nicolet 60SX FTIR spectrometer equipped with both MCT-A and Si diode detectors, KBr and quartz beam-splitters. For measurements in the 500–600 nm α-band of cyt, the sample as well as the Si detector were protected by a blue filter and the sample was illuminated with red actinic light ($\lambda \geq$715 nm). FTIR light-induced spectra of c_{559}^+ were obtained under steady-state continuous illumination, the c_{556}^+ and c_{552}^+ states were photogenerated by flash excitation, using an Nd YAG laser pulse (7 ns, 530 nm). Cycles of illumination were repeated several hundred times.

3. RESULTS

3.1. c_{559} *photooxidation*

For isolated *Rps. viridis* RC, in the absence of reductants and mediators, only c_{559} is at least partially reduced [2] and sub-saturating steady-state illumination causes the predominant photooxidation of this heme. This is due to the fact that the back-reaction between c_{559}^+ and Q_A^- is about two orders of magnitude slower than between P^+ and Q_A^- [11,12]*.

Fig. 1a shows the light-minus-dark FTIR difference spectrum obtained at 10°C under continuous illumination of RC containing *o*-phenanthroline as inhibitor of the Q_A^- to Q_B electron transfer. Fig. 1b shows the light-minus-dark FTIR spectrum generated upon steady-state illumination of RC in the presence of diaminodurene, sodium ascorbate and *o*-phenanthroline. In these conditions where the native electron donors are rapidly reduced by the external donors, it has been previously demonstrated that photochemical generation of the pure Q_A^-/Q_A state occurs, with the three positive bands at 1478 cm^{-1}, 1438 cm^{-1} and 1392 cm^{-1} assigned to the semiquinone anion state while the 1675 cm^{-1}, 1651 cm^{-1}, 1336 cm^{-1} and 1296 cm^{-1} bands are associated with the neutral Q_A state [18,21]. While at first sight, the spectrum in Fig. 1a is dominated by the Q_A^-/Q_A bands, it also shows additional signals. Evidence for Q_A^- formation in Fig. 1a is further demonstrated by the light- minus-dark spectrum in the near-IR (insert A). This difference spectrum has been assigned to electrochromic shifts, mostly of the intermediary bacteriopheophytin electron acceptor, in response to the negative charge on Q_A [11]. For the same RC sample, the insert B of Fig. 1a shows the light-induced difference spectrum in the VIS region where the α-band of each of the 4 hemes displays different spectral characteristics. This spectrum has a negative and narrow peak at 558.5 nm (half-width $\approx$ 8 nm) with a small shoulder at $\approx$ 553 nm, typical of the c_{559} absorption change upon oxidation [2]. These VIS and near-IR controls provide compelling evidence for an assignment of the IR spectral features observed in Fig. 1a to the state $c_{559}^+Q_A^-/c_{559}Q_A$. Fig. 2a is obtained from the calculated difference between spectra of Fig. 1a and 1b after normalization on the Q_A anion bands. The spectrum 2a is thus assigned to the c_{559}^+/c_{559} state. The largest IR absorption changes are observed in the 1620–1700 cm^{-1} (mainly amide I) and 1510–1600 cm^{-1} (amide II, heme modes, ionized carboxyl groups) frequency regions. We estimate that a contamination by P^+/P species (as monitored by the typical P^+ IR band at $\approx$ 1305 cm^{-1} [see 14,22] as well as by the extent of the bleaching of the 960 nm band characteristic of P^+) cannot exceed 2% of the signal displayed on Fig. 2a. The reproducibility of such calcu-

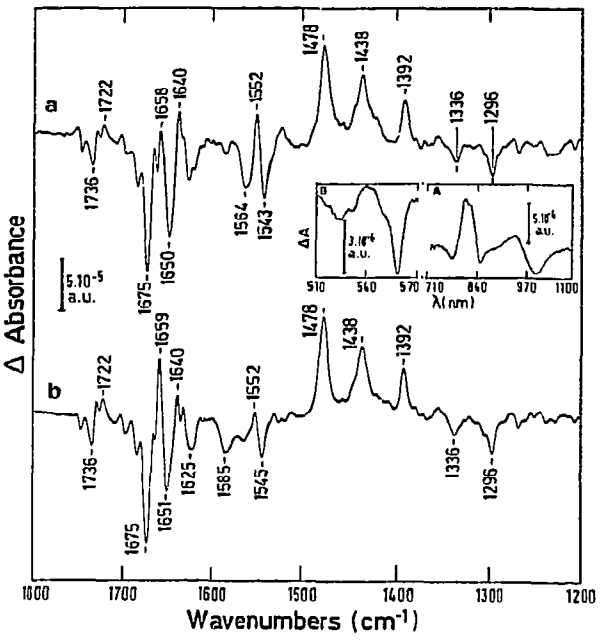

Fig. 1. (a) Light-induced FTIR difference spectrum of *Rps. viridis* RC in the presence of 5 mM *o*-phenanthroline, $\lambda \geq$715 nm, 40960 interferograms co-added. Insert: light-induced difference spectra (A) in the near-IR, 7680 interferograms co-added and (B) in the VIS, 76800 interferograms co-added. (b) Light-induced FTIR difference spectrum of *Rps. viridis* RC in the presence of 5 mM *o*-phenanthroline, 5 mM diaminodurene and 1 mM sodium ascorbate, $\lambda \geq$715 nm, 48640 interferograms co-added. 10°C; 4 cm^{-1} resolution; a.u., absorbance units.

*In order to record a pure light-induced $P^+Q_A^-/PQ_A$ FTIR spectrum, it is essential that all four hemes are pre-oxidized in the dark, a condition which was controlled in the presence of ferricyanide [14]. On the other hand, a significant contribution from oxidized cytochrome appears to contaminate the $P^+Q_A^-/PQ_A$ spectrum reported in [16]. This can be estimated by comparing the relative amplitude of the $\approx$1305 cm^{-1} band, assigned to a pure P^+ mode [22], relative to the amplitude of the 1478 cm^{-1} band contributed by both P^+ [22] and Q_A^- (Fig. 1b).

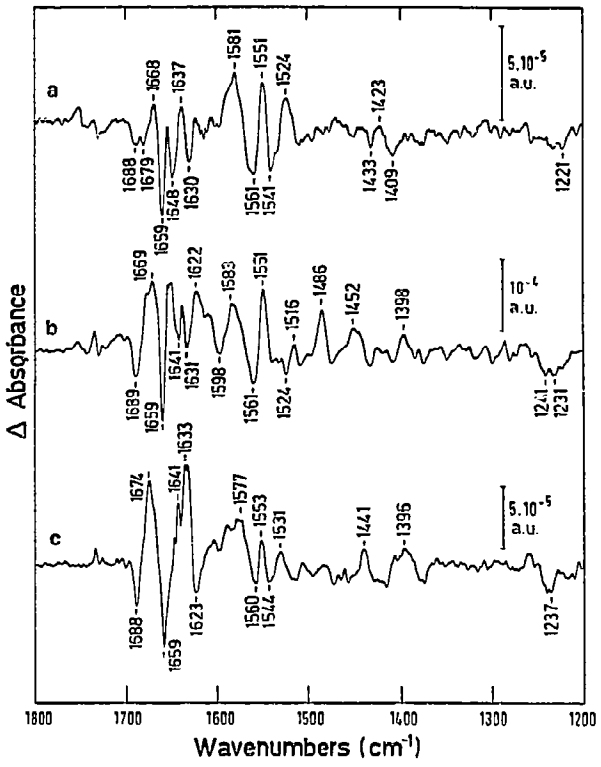

Fig. 2. Comparison of (a) c_{559}^{+}/c_{559}, (b) c_{556}^{+}/c_{556} and (c) c_{552}^{+}/c_{552} FTIR difference spectra obtained after subtraction of the Q_A^-/Q_A spectrum shown on Fig. 1b. The original $cyt^+Q_A^-/cytQ_A$ spectra were first normalized on the amplitude of the Q_A^- anion band at 1478 cm^{-1}. 10°C; 4 cm^{-1} resolution. Interferograms were co-added. (a) 40 960, (b) 14 080 and (c) 38 400. Each peak frequency is given at ±1 cm^{-1}.

lated spectrum has been checked by subtracting different sets of data obtained on either the same or different sample(s). Owing to the noise level observed in these difference spectra, signals of an amplitude larger than 5×10^{-6} to 10^{-5} absorbance unit are considered as significant, depending on the background absorption of the sample. Such a subtraction procedure has already been performed and shown to be reliable on light-induced FTIR spectra of bacteriorhodopsin in order to reveal effects of isotopic labelling of either retinal or amino acids [23,24] and of genetically engineered replacement of amino acids [25].

3.2. c_{556} *photooxidation*

At moderate redox potential c_{556} becomes reduced and the charge-separated state $c_{556}^{+}Q_A^-$ is rapidly created following flash excitation of RC containing only Q_A [12]. This state recombined with a half-time of about 1 s, one order of magnitude slower than the $c_{559}^{+}Q_A^-$ recombination [12]. We have measured the light-induced FTIR difference spectrum for *Rps. viridis* RC in the presence of *o*-phenanthroline and 5 mM sodium ascorbate after excitation by a saturing 7 ns flash. In these conditions, where the delay between the flash and the onset of IR data acquisition was ≈500 ms, any $c_{559}^{+}Q_A^-$ state which could have arisen from a fraction of RC containing c_{556} still oxidized in the dark, recombines too fast to be detected in the IR experiment. The decay of all the bands observed in the light-minus-dark FTIR spectrum (not shown) has a half-time of approx. 2–5 s which is consistent with the charge recombination of $c_{556}^{+}Q_A^-$ [12]. The light-induced FTIR c_{556}^{+}/c_{556} spectrum (after subtraction of the Q_A^-/Q_A spectrum) is displayed on Fig. 2b. Again, the largest IR absorption changes are observed in the 1700–1500 cm^{-1} region. It can already be noticed that the c_{559}^{+}/c_{559} and c_{556}^{+}/c_{556} spectra display several distinct features. The positive band at 1524 cm^{-1} is absent in the c_{556}^{+}/c_{556} spectrum, while additional peaks are observed notably at 1598 cm^{-1}, 1486 cm^{-1}, 1452 cm^{-1} and 1398 cm^{-1} (Fig. 2b). The $c_{556}^{+}Q_A^-/c_{556}Q_A$ state can also be photo-accumulated under steady-state low intensity illumination ($\lambda\geq715$ nm) of RC which have been incubated with 1 mM sodium ascorbate, leading to a spectrum identical to that displayed on Fig. 2b. In these conditions, the photo-induced absorption changes in the VIS show the typical decrease of the cyt α-band at 557 nm (data not shown).

3.3. c_{552} *photooxidation*

Fig. 2c shows the light-minus-dark FTIR spectrum of *Rps. viridis* RC in the presence of *o*-phenanthroline and 30 mM sodium ascorbate following flash excitation and after subtraction of the Q_A^-/Q_A spectrum. In the original $c_{552}^{+}Q_A^-/c_{552}Q_A$ spectrum (data not shown), the bands decay with a half-time of about 2 min in agreement with the slow recombination rate of the $c_{552}^{+}Q_A^-$ state (A.V. and J.B., unpublished). Furthermore, the absence in Fig. 2c of the bands at 1598 cm^{-1} and 1486 cm^{-1} associated with the c_{556}^{+}/c_{556} state (Fig. 2b) shows that contamination of spectrum 2c by c_{556}^{+}/c_{556} can only be very small.

4. DISCUSSION

In light-induced FTIR difference spectra of *Rps. viridis* cytochrome, the identification of individual bands to specific bonds sensitive to the oxidation state involves both protein (backbone and aminoacid side chains) and heme (ring modes and peripheral substituents, i.e. propionic acid) groups. For c_{559}, c_{556} and c_{552}, the most prominent spectral features are observed in the 1700–1500 cm^{-1} frequency range (Fig. 2). Several bands are common to the c_{559}^{+}/c_{559}, c_{556}^{+}/c_{556} and c_{552}^{+}/c_{552} spectra, notably the negative signals at 1659 cm^{-1} and ≈1561 cm^{-1} characterizing the reduced state and the positive signal at ≈1551 cm^{-1} for the oxidized state.

The 1659 cm^{-1} peak lies in the absorption range for peptide C=O of α-helix and could possibly arise from an amino acid localized in the α-helix running parallel to the heme plane [4]. The shape of this band is com-

parable in c_{559}^{+}/c_{559} and c_{556}^{+}/c_{556} spectra while the signal is broader in the c_{552}^{+}/c_{552} spectrum. The amplitude of the 1659 cm^{-1} signal relative to the amplitude of the amide I band suggests that at most one (or possibly two) peptide C=O group(s) could be affected. Thus, it can be concluded that no major rearrangement of the protein backbone accompanies the photooxidation of c_{559}, c_{556} and c_{552} hemes in *Rps. viridis* RC. This conclusion extends previous FTIR spectroelectrochemical studies on cyt *c* from various species [20]. Indeed, comparison of the X-ray structural models of tuna ferro- and ferri-cyt *c* indicates that the largest motions upon oxido-reduction involve localized displacements of a few amino acid side chains surrounding the heme [26,27], thus excluding any large scale alteration in the main chain conformation. In Fig. 2, additional peaks are found in the C=O region such as the negative ones at 1648 cm^{-1} and 1630 cm^{-1} for c_{559}, at 1641 cm^{-1} and 1631 cm^{-1} for c_{556} while large positive signals at 1641 cm^{-1} and 1633 cm^{-1} are observed for c_{552}.

The changes found in the amide I region can be correlated with the presence of peaks in the amide II region (peptide NH bending and CN stretching) at ≈1551 cm^{-1} for the oxidized form, at ≈1561 cm^{-1} for the reduced form. The amplitude of these signals is larger for high-potential hemes than for c_{552}. Therefore, in both the amide I and amide II regions, the c_{552}^{+}/c_{552} spectrum shows differences in the shape and the amplitude of several signals compared to c_{559}^{+}/c_{559} and c_{556}^{+}/c_{556} spectra. This observation is probably related to the slightly different structural organization for c_{552}. The X-ray structural model of the *Rps. viridis* cyt subunit shows a α-helix running parallel to the ring plane of each heme group [4], the hemes being covalently attached near the C-terminal of these helices. However, the sequence homology between the 4 heme-binding domains is low. Only the 2 Cys residues involved in the covalent link to the heme and the subsequent His residue (fifth ligand) are conserved [4]. In addition, the sixth Met ligand to the iron is located within the helix for c_{559} and c_{556} while the corresponding His ligand is in a different part of the structure for c_{552}. Thus, the presence of His as the sixth Fe ligand in c_{552} could induce some structural modification of the polypeptide chain resulting from a change in the environment of the heme.

Contribution from heme modes could also lead to absorption changes in the 1530–1590 cm^{-1} frequency range. An alternative interpretation for the signals observed at ≈1551 cm^{-1}, ≈1561 cm^{-1} and ≈1580 cm^{-1} in Fig. 2 is their assignment to heme C–C ring vibrations. In resonance Raman (RR) spectra of cyt *c*, several bands were identified as being specific for the heme redox state: lines found at 1584 cm^{-1} and 1545 cm^{-1} for the reduced cyt *c*, at ≈1582 cm^{-1} and ≈1561 cm^{-1} for the oxidized state [28,29] have been assigned mostly to C_b–C_b pyrrole stretching vibrations [28–30]. It has also been established that the 1545/1561 cm^{-1} mode is sensitive to the axial ligation at the heme [29]. For example, in the alkylated cyt *c* derivative, where the sixth ligand is changed from Met to Lys [28], this mode which exhibits a pH-dependent frequency shift is observed at 1533 cm^{-1} at high pH in the reduced state. In cyt b_5, where the two axial ligands of the heme iron are histidyl imidazoles, this mode appears at 1538 cm^{-1} [28]. Furthermore, model compound studies using Fe^{2+}-protoporphyrin IX, with the His analogue imidazole occupying both fifth and sixth axial ligand positions, also show an RR line at 1539 cm^{-1} [30]. Little information is available in the literature on the IR modes of heme model compounds [30]. Recently, we have used FTIR spectroelectrochemistry to investigate the redox properties of the (bis)methyl-imidazole complex of Fe-protoporphyrin IX [31]. The most prominent features located at 1552 cm^{-1} and 1535 cm^{-1} for the reduced complex were assigned to heme C_b–C_b modes [31]. Taking into account both sets of RR and IR data, it thus appears most probable that changes in heme C–C vibrations contribute to the IR signals observed in the 1580–1550 cm^{-1} range of c_{559}^{+}/c_{559}, c_{556}^{+}/c_{556} and c_{552}^{+}/c_{552} spectra (Fig. 2). However, no clear IR band assignment can be made with respect to the His-His Fe ligands for c_{552} and His-Met ligands for c_{556} and c_{559}. Furthermore, as already noticed for IR redox-induced difference spectra of heme model compounds [31], the strong RR marker band seen in all *c*-type cyt around 1360 cm^{-1} for the reduced state and around 1375 cm^{-1} for the oxidized state [30] and assigned to the C_a–N stretching mode is not observed in the FTIR difference spectra of either *Rps. viridis* cyt (Fig. 2) or soluble cyt *c* [20]. It can also be noted that the redox-induced IR spectra of various cyt *c* do not show such large signals in the 1580–1550 cm^{-1} region [20], thus suggesting different environments of the hemes for cyt *c* and *Rps. viridis* cyt.

Protonated and unprotonated C=O carboxyl groups usually absorb near 1700–1760 cm^{-1} and 1550–1590 cm^{-1}, respectively [32]. Thus, another possibility for the assignment of the signals at ≈ 1561/1580 cm^{-1} would be to an asymmetric C=O stretch of a carboxylate anion from a heme propionate or a Glu/Asp side chain having different ionic interactions with the protein after oxidation. Signals of an amplitude which we consider just above the noise level in the 1725–1755 cm^{-1} region (Fig. 2) could also possibly involve changes in protonated carboxyl groups of Asp and/or Glu. The absorption of H-bonded C=O from propionic groups is expected below 1700 cm^{-1} [20 and references therein]. In both c_{556}^{+}/c_{556} and c_{552}^{+}/c_{552} spectra (Fig. 2), a negative peak at 1688 cm^{-1} is tentatively assigned to an H-bonded propionic acid group. Negative signals are also observed at 1688 cm^{-1} and 1679 cm^{-1} in c_{559}. In IR difference spectra of cyt *c*, a band at 1693 cm^{-1} seen in the reduced state was assigned to an H-bonded propionic group [20] having an unusually high pK_a [33]. If our

assignment of the 1688 cm^{-1} band in the c_{556} and c_{552} spectra to a propionic is correct, its unusually low frequency indicates a strong H-bonding between the COOH and nearby protein groups, such as the side chains of Tyr^{102}, Tyr^{89} and Arg^{293} for c_{556} and of Gln^{223} for c_{552}.

In proteins, Tyr ring C=C stretch gives rise to a peak at $\approx$1515 cm^{-1} [32]. A common feature to redox-induced IR difference spectra of cyt *c* from several species is the presence of a signal at 1514 cm^{-1} in the reduced state which is shifted to 1518 cm^{-1} after oxidation, giving rise to a sharp and intense differential signal [20]. This characteristic signal was assigned to the C=C ring mode of a redox-sensitive Tyr residue, possibly Tyr^{67} for which cristallographic studies have demonstrated a significant shift in the side chain position between the two redox states [26,27]. Sharp Tyr differential signals have also been recently observed in cyt c_2 from *Rsp. rubrum*, *Rb. sphaeroides* and *Rps. viridis* where a conserved Tyr residue is found in the primary amino acid sequence [34]. The present data demonstrate that the Tyr IR marker is indeed lacking in spectra of *Rps. viridis* cyt (Fig. 2). For c_{559}, c_{556} and c_{552} hemes, at least one Tyr residue belongs to the α-helix running parallel to the heme plane [4,35] although the 3D map of the RC shows that no Tyr lies in the very close proximity of c_{559} and c_{552} hemes. For c_{556}, several Tyr are found near the heme and in particular, Tyr^{102} and Tyr^{89} side chains are within H-bonding distance to the carboxyl group of one propionic. Although we cannot exclude that the small positive signal observed at 1516 cm^{-1} in the c_{556}^{+}/c_{556} spectrum (Fig. 2c) could arise from a change in Tyr C=C vibrations, the absence of the characteristic Tyr marker in all spectra of Fig. 2 provides evidence that the localized shift of a Tyr side chain observed between oxidized and reduced cyt *c*, does not occur in *Rps. viridis* cyt.

In conclusion, the present IR data demonstrate that upon photooxidation of either high-potential (c_{559} and c_{556}) or low-potential (c_{552}) hemes, the overall polypeptide backbone conformation is not affected. In this respect, *Rps. viridis* cyt is similar to cyt *c* [20] in that both show no large conformational change associated with a change of state of the iron. However, significant dissimilarities between oxidized-minus-reduced FTIR spectra of the two systems are most probably related to the structural differences already noticed in X-ray crystallographic studies which indicate that the protein folding in the *Rps. viridis* cyt unit is different from all other cyt of known 3D structure [4,36].

Acknowledgements: The authors acknowledge discussions with W. Mäntele, F. Fritz and F. Baymann.

REFERENCES

[1] Shopes, R.J., Levine, L.M.A., Holten, D. and Wraight, C.A. (1987) Photosynth. Res. 12, 165–180.
[2] Dracheva, S.M., Drachev, L.A., Konstantinov, A.A., Semenov, A.Yu, Skulachev, V.P., Arutjunjan, A.M., Shuvalov, V.A. and Zaberezhnaya, S.M. (1988) Eur. J. Biochem. 171, 253–264.
[3] Deisenhofer, J., Epp, O., Miki, K., Huber, R. and Michel, H. (1984) J. Mol. Biol. 180, 385–398.
[4] Deisenhofer, J., Epp, O., Miki, K., Huber, R. and Michel, H. (1985) Nature 318, 618–624.
[5] Dracheva, S.M., Drachev, L.A., Zaberezhnaya, S.M., Konstantinov, A.A., Semenov, A.Yu. and Skulachev, V.P. (1986) FEBS Lett. 205, 41–46.
[6] Fritzsch, G., Buchanan, S. and Michel, H. (1989) Biochim. Biophys. Acta 977, 157–162.
[7] Verméglio, A., Richaud, P. and Breton, J. (1989) FEBS Lett. 243, 259–263.
[8] Nitschke, W. and Rutherford, A.W. (1989) Biochemistry 28, 3161–3168.
[9] Hubbard, J.A.M. and Evans, M.C.W. (1989) FEBS Lett. 244, 71–75.
[10] Shinkarev, V.P., Drachev, A.L. and Dracheva, S.M. (1990) FEBS Lett. 261, 11–13.
[11] Shopes, R.J. and Wraight, C.A. (1985) Biochim. Biophys. Acta 806, 348–356.
[12] Gao, Ji-L., Shopes, R.J. and Wraight, C.A. (1990) Biochim. Biophys. Acta 1015, 96–108.
[13] Mäntele, W., Wollenweber, A., Nabedryk, E. and Breton, J. (1988) Proc. Natl. Acad. Sci. USA 85, 8468–8472.
[14] Nabedryk, E., Bagley, K.A., Thibodeau, D.L., Bauscher, M., Mäntele, W. and Breton, J. (1990) FEBS Lett. 266, 59–62.
[15] Buchanan, S., Michel, H. and Gerwert, K. (1990) in: Current Research in Photosynthesis, vol. I (M. Baltscheffsky, ed.) pp. 69–72, Kluwer Academic Publishers, Dordrecht.
[16] Buchanan, S., Michel, H. and Gerwert, K. (1990) in: Reaction Centers of Photosynthetic Bacteria (Michel-Beyerle, M.-E., ed.) pp. 75–85, Springer Verlag, Berlin.
[17] Thibodeau, D.L., Breton, J., Berthomieu, C., Bagley, K.A., Mäntele, W. and Nabedryk, E. (1990) in: Reaction Centers of Photosynthetic Bacteria (Michel-Beyerle, M.-E., ed.) pp. 87–98, Springer Verlag, Berlin.
[18] Breton, J., Thibodeau, D.L., Berthomieu, C., Mäntele, W., Verméglio, A. and Nabedryk, E. (1991) FEBS Lett. 278, 257–260.
[19] Breton, J., Berthomieu, C., Thibodeau, D.L. and Nabedryk, E. (1991) FEBS Lett. 288, 109–113.
[20] Moss, D., Nabedryk, E., Breton, J. and Mäntele, W. (1990) Eur. J. Biochem. 187, 565–572.
[21] Breton, J., Bauscher, M., Berthomieu, C., Thibodeau, D., Andrianambinintsoa, S., Dejonghe, D., Mäntele, W. and Nabedryk, E. (1991) in: Spectroscopy of Biological Molecules (R.E. Hester and R.B. Girling, eds.) pp. 43–46, The Royal Society of Chemistry, Cambridge.
[22] Leonhard, M., Moss, D., Bauscher, M., Nabedryk, E., Breton, J. and Mäntele, W. (1991) in: Spectroscopy of Biological Molecules (R.E. Hester and R.B. Girling, eds.) pp. 75–76, The Royal Society of Chemistry, Cambridge.
[23] Gerwert, K. and Siebert, F. (1986) EMBO J. 5, 805–811.
[24] Gerwert, K., Hess, B. and Engelhard, M. (1990) FEBS Lett. 261, 449–454.
[25] Gerwert, K., Hess, B., Soppa, J. and Oesterhelt, D. (1989) Proc. Natl. Acad. Sci. USA 86, 4943–4947.
[26] Takano, T. and Dickerson, R.E. (1981) J. Mol. Biol. 153, 95–115.
[27] Bushnell, G.W., Louie, G.V. and Brayer, G.D. (1990) J. Mol. Biol. 214, 585–595.
[28] Kitagawa, T., Kyogoku, Y., Iizuka, T., Ikeda-Saito, M. and Yamanaka, T. (1975) J. Biochem. 78, 719–728.
[29] Kitagawa, T., Ozaki, Y., Teraoka, J., Kyogoku, Y. and Yamanaka, T. (1977) Biochim. Biophys. Acta 494, 100–114.
[30] Choi, S., Lee, J.J., Wei, Y.H. and Spiro, T.G. (1983) J. Am. Chem. Soc. 105, 3692–3707.
[31] Berthomieu, C., Moss, D., Mäntele, W., Boussac, A., Breton, J. and Nabedryk, E. (1991) in: Spectroscopy of Biological Mole-

cules (R.E. Hester and R.B. Girling, eds.) pp. 83–84, The Royal Society of Chemistry, Cambridge.
[32] Venyaminov, S., Yu. and Kalnin, N.N. (1991) Biopolymers 30, 1243–1257.
[33] Hartshorn, R.T. and Moore, G.R. (1989) Biochem. J. 258, 595–598.
[34] Baymann, F. (1991) Diplomat Thesis, Faculty of Biology, University of Freiburg, Germany.
[35] Weyer, K.A., Lottspeich, F., Gruenberg, H., Lang, F., Oesterhelt, D. and Michel, H. (1987) EMBO J. 6, 2197–2202.
[36] Mathews, F.S. (1985) Prog. Biophys. Mol. Biol. 45, 1–56.